



Published in final edited form as:

Clin Cancer Res. 2012 April 15; 18(8): 2240–2249. doi:10.1158/1078-0432.CCR-11-2654.

Improved efficacy of dendritic cell-based immunotherapy by cutaneous laser illumination

Xinyuan Chen[§], Qiyan Zeng[§], and Mei X. Wu^{§,*,#}

[§]Wellman Center for Photomedicine, Massachusetts General Hospital (MGH), Department of Dermatology, Harvard Medical School (HMS), Boston, MA

[#]Harvard-MIT Division of Health Sciences and Technology (HST), Cambridge, MA

Abstract

Purpose—The present investigation demonstrates a convenient laser-based approach to enhance DC migration resulting in improved DC-based immunotherapy in murine models.

Experimental design—Influence of laser illumination on dermal tissue microenvironment and migration of DCs following intradermal injection were determined by whole-mount immunohistochemistry, transmission electron microscope, and flow cytometry. We also investigated *in vivo* expansion of cytotoxic T lymphocytes (CTLs) by flow cytometry, CTL activity by *in vitro* CTL assay, and anti-tumor efficacy of DC immunization following cutaneous laser illumination in both preventive and therapeutic tumor models.

Results—Laser illumination was found to significantly enlarge perforations in the peri-lymphatic basement membrane, disarray collagen fibers and disrupt cell-matrix interactions in the dermis. The altered dermal tissue microenvironment permitted more efficient migration of intradermally injected DCs from the dermis to the draining lymph nodes (dLNs). Laser illumination also slightly but significantly enhanced the expression of costimulatory molecule CD80 and MHC I on DCs injected into the skin, when compared to those DCs administered into sham-treated skin. As a result, more vigorous expansion of tumor-specific IFN- γ ⁺CD8⁺ T lymphocytes and enhanced CTL activity against 4T1 but not irrelevant tumor cells were obtained in the laser-treated group over the control group. Laser-augmented DC immunization also completely abrogated early growth of 4T1 tumor and B16F10 melanoma in preventive tumor models and significantly extended the survival of 4T1-resected mice in a therapeutic tumor model.

Conclusion—These data suggest a simple, safe, laser-based approach to significantly enhance DC-based immunotherapy.

Keywords

dendritic cell; migration; maturation; tumor; immunotherapy; laser

Introduction

With the ability of generating large amounts of dendritic cells (DCs) *ex vivo* in the past two decades, therapeutic potential of DCs has been extensively explored in preclinical and clinical studies, in particular, in the field of tumor immunotherapy^{1–3}. In the clinic, DCs can be generated from human peripheral blood monocytes, matured in the presence of

Address Correspondence to: Mei X. Wu, Wellman Center for Photomedicine, Massachusetts General Hospital, 50 Blossom Street, Edwards 222, Boston, MA 02114, TEL: 617-726-1298; FAX: 617-726-1208; mwu2@partners.org.

The authors have no conflict of interest to declare.

appropriate growth factors and cytokines, pulsed with tumor antigens, and given back to patients to elicit anti-tumor immunity^{1, 3}. This DC-based immunotherapy has been broadly evaluated in a variety of tumors, like malignant melanoma, prostate cancer, breast cancer, renal cell carcinoma, and so on^{3, 4}. However, only a small fraction (<1%) of DCs could migrate to the draining lymph nodes (dLNs) following intradermal (*i.d.*) or subcutaneous (*s.c.*) injection and the majority of DCs remained and died over time at the site of injection, limiting their anti-tumor efficacy^{3, 5}. A novel strategy to improve DC migration from the skin to the dLNs would potentially boost DC-based immunotherapy.

In the skin, initial lymphatic vessels (LVs) are localized beneath the epidermis and serve as a conduit for DC migration from the skin to the dLNs. Migration of DCs to and through the LVs after *i.d.* administration is primarily guided by chemokine gradients of CCL19/CCL21 secreted by lymphatic endothelial cells under a physiological condition⁶. Apart from chemokines, gene knockout studies indicate that intrinsic DC migratory ability and dermal tissue microenvironment are also pivotal in the control of DC migration from the skin to the dLNs. In this regard, a lack of major histocompatibility complex (MHC) II-associated invariant chain (Ii or CD74) or junctional adhesion molecular A (JAM-A) on DCs was associated with increased DC motility *in vitro* and sufficient migration of the cells to the dLNs *in vivo* due to decreased adhesion to the matrix of the skin connective tissue^{7, 8}. In contrast, absence of metalloproteinase (MMP)-2 and -9 on DCs diminished their ability to degrade extracellular matrix proteins, resulting in reduced DC migration to the dLNs after *s.c.* injection^{9, 10}. An importance of dermal tissue microenvironment in the control of DC migration was also stressed by deletion of a matricellular protein named SPARC (secreted protein, acidic, rich in cysteine, or osteonectin/BM-40). Bone marrow (BM)-derived DCs migrated more sufficiently to the dLNs in SPARC-deficient mice than in wild type mice following *i.d.* injection¹¹.

The dermal connective tissue consists of densely aligned collagen fibers and extracellular matrixes that serve as tissue scaffold restricting DC migration. We recently developed a laser-based vaccine adjuvant capable of safe and efficient enhancement of vaccine-induced immune response¹². The vaccine adjuvant effect is induced primarily by enhancing velocity and motility of *in situ* DCs in the skin as well as sufficient transportation of antigen-captured DCs from the immunization site to the dLNs. In the present study, we demonstrate that the laser illumination can also greatly enhance migration of *i.d.* injected DCs to the dLNs and potentiate DC-based immunotherapy in both preventive and therapeutic tumor models.

Materials and methods

Mice

BALB/c mice at 6–8 weeks of age were purchased from Charles River Laboratories (Wilmington, MA). C57BL/6 (B6, CD45.2) and B6.SJL (CD45.1) mice at 6–8 weeks were purchased from the Jackson Laboratory (Bar Harbor, ME). MHC II-EGFP mice expressing MHC class II molecule infused into enhanced green fluorescent protein (EGFP) were a kindly gift of Drs. Boes and Ploegh, Department of Pathology, Harvard Medical School¹³. All mice were housed in conventional cages at the animal facilities of Massachusetts General Hospital in compliance with institutional guidelines. All animal procedures were reviewed and approved by the Subcommittee on Research Animal Care at the Massachusetts General Hospital.

Laser Devices

A Q-switched 532-nm Nd:YAG laser (Spectra-Physics Inc., Mountain View, CA) was used with a pulse width 6ns, a beam diameter ~7 mm, and a frequency 10Hz. The average output

power was measured by a power meter (Ophir Optics, Inc., MA) and temperature (T_m) at the illumination center of the skin was monitored by an infrared camera (FLIR Systems, Boston, MA).

DC generation and CFSE labeling

BM-derived DCs were prepared as described¹⁴. Briefly, femur and tibia BM cells were cultured for 6 days in the presence of recombinant murine GM-CSF (15ng/ml) and IL4 (10ng/ml). Non-adherent cells were re-plated and matured by recombinant murine TNF- α (50ng/ml) and LPS (100ng/ml) for another 2 days. Mature DCs (mDCs) were harvested on day 8 and stained for 20 min at 37°C with 10 μ M CFSE [5-(and-6)-carboxyeosin diacetate, succinimidyl ester] (Invitrogen, Carlsbad, CA) according to the manufacturer's instruction. GM-CSF, IL4, and TNF- α were all purchased from R & D Systems (Minneapolis, ME) and LPS was obtained from Sigma (St. Louis, MO).

DC migration and maturation

CFSE-labeled DCs were *i.d.* injected to the lower dorsal skin of mice and dLNs were collected at indicated times after DC administration. Single cell suspensions were prepared as our previous report¹² and stained with PE-anti-cd11c (N418), PerCP-Cy5.5-anti-CD45.2 (104) or APC-anti-CD45.1 (A20) followed by flow cytometric analysis on BD FACSAria. Migrated DCs marked as CFSE⁺ cd11c⁺ cells were calculated relatively to the total cell number of the lymph node. To analyze DC maturation, DCs were stained with PE-anti-CD80 (16-10A1), APC-anti-MHC II (M5/114.15.2), PE-anti-MHC I (28-8-6), and APC-anti-CD40 (3/23) and subjected to flow cytometry analysis of mean fluorescence intensity (MFI) of CD80, MHC II, CD40, and MHC I expression in gated CFSE⁺ cd11c⁺ cells.

DC pulsing and immunization

Autologous tumor lysates were used to pulse mDCs¹⁵. Briefly, 4T1 breast tumor cells (ATCC, CRL-2539) and renal adenocarcinoma cells (Renca, ATCC, CRL-2947) were cultured in RPMI 1640 and B16F10 melanoma cells (ATCC, CRL-6475) were cultured in DMEM. The culture media were supplemented with 10% FBS, 2 mM L-glutamine, and 1% penicillin-streptomycin. The cells were harvested and subjected to 4 freeze-thaw cycles followed by centrifugation at 5,000 rpm for 30 min. Supernatants were collected and added to the DC culture for 18 hrs in a tumor to DC ratio of 3:1. Tumor lysate-pulsed mDCs (5×10^5) were *i.d.* injected into syngeneic BALB/c or C57BL/6 mice at the site of laser illumination (0.4W for 1.5 minutes except otherwise specified) right after laser treatment or a corresponding sham site once a week for three consecutive weeks.

Tumor inoculation, resection, and metastases

4T1 cells (3×10^4) and B16F10 (5×10^4) per mouse were *s.c.* inoculated to the right flank of BALB/c and C57BL/6 mice, respectively. Tumor volume measurement and tumor resection were referred to our previous report¹⁶. Lung metastatic foci were counted under a dissection microscope by an investigator blind to the sample groups after careful dissection and separation of the lung tissue into single lobes.

Statistical analysis

Student *t*-test and one-way ANOVA were used to analyze a difference between two groups or among multiple groups, respectively. Kaplan-Meier method and log-rank test were used to analyze the survival data. *p* values were calculated by PRISM software (GraphPad, San Diego, CA) and considered significant if a *p* value was less than 0.05.

Additional methods and materials can be found in online supplements including whole-mount ear immunofluorescent staining, transmission electron microscopy (TEM), CTL assays, and intracellular cytokine staining.

Results

Laser enhances lymphatic entry of *in situ* antigen presenting cells (APCs)

Our previous study showed that cutaneous laser illumination at a specific setting increased the motility of APCs in the skin without incurring any overt side effects¹². To address how the increased motility affected lymphatic transportation of the cells, the right ear of MHCII-EGFP transgenic mice was exposed to laser at 80mW for 15 seconds, a low laser dose that is well tolerable to the ear, followed by intravital confocal imaging one hr later as previously described¹². We found a number of dermal cords in the laser-illuminated area but not in the control ear, presumably resulting from a high number of GFP⁺ cells flowing into lymphatic vessels (LVs) (figure 1A). These GFP⁺ cells encompass mainly MHC class II⁺ DCs and macrophages defined broadly as APCs^{13, 17}. Confocal imaging of collagen IV-stained whole-mount ear of MHC II-EGFP transgenic mice revealed few, if any, GFP⁺ cells inside the LVs under a physiological condition (figure 1B). Enumeration of ~250 GFP⁺ cells in 15 randomly selected fields found only 0.8% GFP⁺ cells inside LVs in control ear, which increased by 20-fold, 30 min after laser illumination (figures 1B–C). Meanwhile, percentage of GFP⁺ cells in association with the lymphatic vessel wall was increased from 10.9% in control ear to 38.2% in laser-illuminated ear (figures 1B–C). These LV-associated cells crawled on the vessel wall and some of them extended their body into the channel (figure 2A). In contrast, few GFP⁺ cells crawled or extended their body into the channel in the control ear (figure 1A, 2A). Moreover, laser illumination appeared to enlarge pre-formed portals in peri-lymphatic membrane as previously described¹⁸. The average diameter of the channels was $1.57 \pm 0.06 \mu\text{m}$ in the control ear but $2.93 \pm 0.20 \mu\text{m}$ after laser illumination, a representative of an 87% increase (figure 2A–B). The size of the channels was further enlarged to $4.34 \pm 0.29 \mu\text{m}$ with cell occupancy, corroborating previous investigation showing that the preformed channels could be passively dilated by entering cells¹⁸.

We next investigated whether laser illumination also disarrayed the densely packed dermal connective tissue, permitting relatively free cell migration in the interstice. To this end, transmission electron microscopy (TEM) was used to analyze the ultra-structure of the dermis following laser illumination at 0.3W for 2 min. Dermal connective tissue was comprised of well-aligned bundles of collagen fibers in control skin and the cells were intimately contacted and surrounded with dense extracellular matrix and fibers with which cell migration might be restricted (figure 2C). Upon laser illumination, however, dermal tissue became loosely compacted with apparent gaps between fibers and between fibers and cells. The cells in laser-illuminated skin were disconnected with collagen fibers, concurrent with extending their long dendrites to remote fibers, suggestive of cell migration. These data, in line with our previous investigation¹², suggest that laser facilitates DC migration from the skin to the LVs potentially by at least three mechanisms: enlargement of the preformed channels in the initial LVs, disarray of the dense protein network, and increased motility of APCs.

Laser enhances DC migration and their maturation following *i.d.* injection

Laser-induced alterations in the dermal microstructure described above promoted us to investigate whether cutaneous laser illumination could enhance migration of *i.d.* injected DCs to the dLNs. As shown in figure 3A and 3B, laser illumination significantly increased the number of DCs migrating into the dLNs at all times tested, with cumulative migration peaking on day 2 after DC inoculation. At the peaking level, the inoculated DCs arriving at

the dLN increased from 1376 ± 176 in control group to 2735 ± 256 in 0.3W laser group or 3482 ± 188 in 0.4W laser group in BALB/c mice, or from 1668 ± 100 in control group to 2947 ± 210 in 0.3W laser group or 3738 ± 262 in 0.4W laser group in C57BL/6 mice (figure 3C). No CFSE+ DCs were found in the dLNs of PBS-injected control mice (data not shown). Besides mDCs, laser also enhanced migration of immature DCs similarly (data not shown), in agreement with a physics-, rather than chemokine-, involved mechanism in laser-augmented migration of DCs. The migration efficiency appeared to be laser power-dependent with laser illumination at 0.4W for 1.5 min significantly stronger than that at 0.3W for 2 min in both mice and thus laser illumination at 0.4 W for 1.5 min was chosen in the subsequent studies. In addition to DC migration, how laser illumination affected the maturation of *i.d.* injected mDCs was also evaluated two days after DC injection. As shown in figure 3D, MFIs of CD80 and MHC-1 expression, but not of CD40 and MHC II expression on injected DCs were slightly but significantly higher in laser-treated skin than in sham-treated skin. The result suggests that laser illumination doesn't compromise, but augments DC maturation following *i.d.* injection even though the micro-architecture of the skin connective tissue is significantly altered by laser exposure.

Laser expands CD8+ T cells and increases Cytotoxic T lymphocyte (CTL) activity

To address whether laser-enhanced DC migration gave rise to more vigorous CD8+ T cell responses, the number and function of these cells were evaluated one week after the last immunization. It was found that the percentage of IFN γ -secreting CD8+ T cells relative to a total number of CD8+ T cells was $1.12 \pm 0.15\%$ in control group, but increased to $3.32 \pm 0.31\%$ in DC group, or 4.73 ± 0.08 in laser+DC group, which represents a 42% increase in the presence as compared to the absence of laser illumination (figure 4A–B). Similarly, the total number of IFN γ -secreting CD8+ T cells per LN was 2.3-fold higher with laser than without it ($p < 0.001$, figure 4C) and this trend was extended to the spleen (figure 4D). No significant increases were seen in the number of IL4- or IFN γ -secreting CD4+ T cells or IL4-secreting CD8+ T cells by laser illumination in spite of the slightly high levels of their induction as compared to control groups (data not shown). Furthermore, T cells isolated from mice immunized with 4T1-tumor lysate-pulsed mDCs showed specific killing of 4T1 tumor cells, but not irrelevant Renca cells, with the killing activity significantly stronger in the presence than in the absence of laser illumination (figure 4E–F). These results strongly suggest that laser illumination followed by DC immunization selectively expands tumor specific IFN γ -secreting CD8+ T cells and increases their specific cytotoxicity.

Laser enhances efficacy of DC-based immunotherapy

We next validated whether more vigorous expansion of tumor-specific CD8+ T cells and enhanced CTL activity could be translated into enhanced anti-tumor immunity. As shown in figure 5A, no 4T1 tumor growth was seen for 17 days after tumor inoculation in laser+DC group. In sharp contrast, tumor grew fast in the control and DC groups: tumor volume reached 131 mm^3 in control group and 64 mm^3 in DC group on day 17. The tumor in laser +DC group gradually became visible thereafter and was 150 mm^3 4 weeks after tumor inoculation, whereas tumor was 637 mm^3 in control group and 399 mm^3 in DC group at the same time. At the end of the study, tumor mass was 74% smaller in mice receiving DC immunization at the site of laser illumination or 40% smaller in mice receiving DC immunization alone than that in non-immunized mice ($p < 0.01$, figure 5B). Moreover, laser plus DC immunization reduced lung metastases significantly, as manifested by significantly fewer lung metastatic foci when compared to control group ($p < 0.05$, figure 5C). No significant difference was found in lung metastatic foci between control and DC immunization alone under similar conditions. No macroscopic metastases were found in other organs like liver, kidney, intestine, colon, and brain. Laser-mediated improvement of DC-based immunotherapy was also demonstrated with B16F10 melanoma in C57BL6 mice.

All mice in control group (6/6) and two-thirds of the mice in DC group (4/6) developed visible tumors within 2 weeks, while none of the mice in laser+DC group (0/6) developed tumor in the entire experimental period (figure 5D). Log-rank test indicated that the percentage of tumor-free mice in laser+DC group was significantly higher than all other groups ($p < 0.05$ vs. DC group and $p < 0.001$ vs. control group). In accordance with this, tumor volume on average was significantly smaller in laser-treated group than in sham-treated group (figure 5E). Strikingly, while DC immunization reduced tumor volume, laser plus DC immunization completely abrogated tumor growth in the entire observation period. All mice in control and laser+unpulsed DC groups, and 4 out of 6 mice in DC group, died of cancer within 50 days, but all mice in laser+DC group survived beyond the end of the experiment ($p < 0.001$ vs. control group; $p < 0.05$ vs. DC group). Laser-enhanced DC immunotherapy in both 4T1 and B16F10 models critically depended on tumor antigen used to pulse DCs since no significant protection was attained when unpulsed DCs were administered into the site of laser illumination (figure 5A–F, Laser+unpulsed DC).

Laser extends the survival of tumor-resected mice

DC-based immunotherapy would be most valuable in prevention of tumor relapse or tumor resection-induced metastases for patients with primary tumor surgically removed. In an attempt to mimic this clinic setting, BALB/c mice were *s.c.* inoculated with 4T1 tumor cells and primary tumor was surgically removed after reaching 100 mm³. One week later, tumor-resected mice were *i.d.* immunized with tumor lysate-pulsed mDCs at the site of laser or sham illumination once a week for three weeks. All mice in control and DC groups succumbed to severe lung metastases within 28 days after tumor resection. In contrast, 50% of the mice in laser+DC group were still alive at this time point, although the mice eventually died in the following weeks. Log-rank test verified that laser plus DC, but not DC alone, significantly extended the survival of tumor-resected mice ($p = 0.017$ vs. control group and $p = 0.042$ vs. DC group, figure 6), suggesting brief laser illumination prior to DC immunization could give rise to more effective therapy.

Discussion

The present investigation introduces a novel technology to improve DC-based immunotherapy by using cutaneous laser illumination to enhance DC migration following *i.d.* injection. We observe dermal cord formation in MHC-II-EGFP mice within one hr after laser illumination, which, to the best of our knowledge, is the first report on the visualization of *in vivo* dermal cord formation. Active entry of skin APCs into LVs was seen 30 min after laser illumination, in contrast to dermal cord formation in *ex vivo* skin explants that occurs after 1–3 days of culture in a manner dependent on maturation and chemoattraction of APCs^{19–22}. The observation argues that laser illumination induces dermal cord formation by a different mechanism since synthesis and release of CCL19/CCL21 chemokines by lymphatic endothelial cells takes at least 6–8 hrs^{23, 24}. Moreover, when immature DCs were administered into the site of laser illumination, similar enhancement in DC migration from the skin to the dLNs was also observed (data not shown). These immature DCs did not express a significant level of the CCR7 receptor, a chemokine receptor for CCL19/CCL21, on the surface and laser-treated skin did not produce detectable levels of CCL19/CCL21 chemokines either at this time point when measured by real time RT-PCR in homogenates prepared from the skin (data not shown). This chemokine-independent, instant effect of laser on DC migration would be significant in the clinic where laser illumination and DC administration can be performed at the same visit. In contrast, utilization of TNF α or imiquimod to enhance DC migration requires more than 6 hr-treatment of the injection site before DC administration. In addition, laser illumination could enhance DC migration similarly and significantly in a broad dose range from 10⁵ to 10⁶ cells injected, which would be a key because 10⁶ DCs are usually needed for effective DC-based immunotherapy²⁵.

Unlike laser illumination, the efficacy of inflammatory cytokine-enhanced DC migration varied with the number of DCs, with a maximal effect when less than 5×10^5 DCs were injected and a minimal effect if more than 10^6 DCs were injected²⁴. Repeated imiquimod treatment of DC injection site has been reported to synergize with DC-based immunotherapy in an intracranial tumor model by increasing migration and survival of injected DCs and enhancing priming of tumor-specific CD8+ T cells²⁶. While the effect of laser illumination is similar to repeated imiquimod treatment in enhancement of DC migration, expansion of tumor-specific CD8+ T cells, and inhibition of tumor growth, single laser treatment is much more convenient when compared with multiple imiquimod treatments at different time points. Further studies are needed to determine whether combination of laser with imiquimod can further enhance DC-based immunotherapy.

One mechanism underlying laser-facilitated DC migration may be alterations of the dermal micro-architecture, such as loosely compacted dermal tissues, enlarged gaps, and disarrayed collagen fibers, as suggested by the TEM study. These alterations would reduce DC migratory resistance in the interstice and increase DC motility as shown in our previous study¹². It is also clear that laser illumination results in significant enlargement of preformed channels in the basement membrane of the initial LVs¹⁸, adding another attributable factor to a sufficient entrance of DCs into the LV. Moreover, it is well known that fever can accelerate interstitial flow by 10-fold and promote lymphatic transportation of APCs during infection^{27, 28}. Although it has not been tested, increased interstitial flow presumably contributes to the effect as well, since local skin temperature was increased to 41°C when measured by an infrared camera focusing on the center of the illumination site. A pulsed temperature inside the skin may be higher at its peak as a high-repetition short pulsed laser was used²⁹, although further investigation is required to unravel the photothermal effect. Besides, we found by injection of mDCs from congenic B6.SJL mice into C57BL/6 mice that CFSE+cd11c+ cells in the dLNs were primarily the injected CD45.1+ DCs, not CD45.2 host cells that took up of CFSE-stained cells, ruling out that skin resident DCs were activated after engulfment of CFSE-stained DCs and migrated into the dLNs, contributing to the observed therapeutic improvement. The finding is consistent with little improvement of DC-based immunotherapy when laser illumination was followed by injection of unpulsed DCs. In brief, our data suggest that laser-augmented migration of DCs involves a complex physical mechanism, which is consistent with the quick formation of dermal cords after laser illumination and its independence of DC maturation status.

DC-based immunotherapy has been extensively evaluated in the clinic in a variety of tumor models in the past two decades. However, it is until very recently that this approach shows significantly prolonging patient survival with advanced prostate cancer and melanoma^{30, 31}. But the efficacy is far from satisfying, requiring improvement in multi-facets, among which the major efforts have been made to optimize DC culture conditions, cytokine cocktails for maturation, and tumor antigen loading. Laser modulation of the skin at the injection site to enhance DC migration can be complementary to any of these efforts to further improve therapeutic efficacy of DCs. Although intravenous (*i.v.*) infusion is also used to deliver therapeutic DCs in the clinic, this route of administration has been found to favor humoral immune response, rather than cell-mediated immune response that is more pivotal for tumor therapy^{3, 32-34}. In addition, *i.v.* delivery of DCs induced memory T cells primarily in the spleen, whereas *i.d.* route of DC delivery induced memory T cells not only in the spleen but also in the lymph nodes, enabling more target protection against tumors at specific anatomic locations like cutaneous tumors and breast cancer in which metastatic tumor cells first reach cutaneous lymph nodes^{3, 35}. Furthermore, because laser only illuminates a small area of the skin, this procedure is unlikely to generate any undesirable systemic side effects, it is expected to gain fast approval by FDA, and it thus warrants further investigation.

Supplementary Material

Refer to Web version on PubMed Central for supplementary material.

Acknowledgments

The authors would like to thank Dakai Mu and Zhanliang Wei for harvesting and culturing of BM-derived DCs, Peggy Sherwood for TEM sectioning, staining, and picture taking, the member in Drs. Wu's groups for stimulating discussion, Drs Boes and Ploegh for MHC-II-EGFP mice.

Financial Support: This work is supported in part by the National Institutes of Health grants AI070785 and RC1 DA028378, and Grand Challenges Explorations grant # 53273 from the Bill and Melinda Gates Foundation (to M.X.W.).

Reference List

1. Figdor CG, de Vries IJ, Lesterhuis WJ, Melief CJ. Dendritic cell immunotherapy: mapping the way. *Nat Med.* 2004; 10:475–480. [PubMed: 15122249]
2. Tacken PJ, de Vries IJ, Torensma R, Figdor CG. Dendritic-cell immunotherapy: from ex vivo loading to in vivo targeting. *Nat Rev Immunol.* 2007; 7:790–802. [PubMed: 17853902]
3. Banchereau J, Palucka AK. Dendritic cells as therapeutic vaccines against cancer. *Nat Rev Immunol.* 2005; 5:296–306. [PubMed: 15803149]
4. Zitvogel L, Angevin E, Tursz T. Dendritic cell-based immunotherapy of cancer. *Ann Oncol.* 2000; 11 (Suppl 3):199–205. [PubMed: 11079142]
5. Palucka AK, Ueno H, Fay J, Banchereau J. Dendritic cells: a critical player in cancer therapy? *J Immunother.* 2008; 31:793–805. [PubMed: 18833008]
6. Randolph GJ, Angeli V, Swartz MA. Dendritic-cell trafficking to lymph nodes through lymphatic vessels. *Nat Rev Immunol.* 2005; 5:617–628. [PubMed: 16056255]
7. Faure-Andre G, Vargas P, Yuseff MI, Heuze M, Diaz J, Lankar D, et al. Regulation of dendritic cell migration by CD74, the MHC class II-associated invariant chain. *Science.* 2008; 322:1705–1710. [PubMed: 19074353]
8. Cera MR, Del Prete A, Vecchi A, Corada M, Martin-Padura I, Motoike T, et al. Increased DC trafficking to lymph nodes and contact hypersensitivity in junctional adhesion molecule-A-deficient mice. *J Clin Invest.* 2004; 114:729–738. [PubMed: 15343392]
9. Yen JH, Khayrullina T, Ganea D. PGE2-induced metalloproteinase-9 is essential for dendritic cell migration. *Blood.* 2008; 111:260–270. [PubMed: 17925490]
10. Ratzinger G, Stoitzner P, Ebner S, Lutz MB, Layton GT, Rainer C, et al. Matrix metalloproteinases 9 and 2 are necessary for the migration of Langerhans cells and dermal dendritic cells from human and murine skin. *J Immunol.* 2002; 168:4361–4371. [PubMed: 11970978]
11. Sangaletti S, Gioiosa L, Guiducci C, Rotta G, Rescigno M, Stoppacciaro A, et al. Accelerated dendritic-cell migration and T-cell priming in SPARC-deficient mice. *J Cell Sci.* 2005; 118:3685–3694. [PubMed: 16046482]
12. Chen X, Kim P, Farinelli B, Doukas A, Yun SH, Gelfand JA, et al. A novel laser vaccine adjuvant increases the motility of antigen presenting cells. *PLoS One.* 2010; 5:e13776. [PubMed: 21048884]
13. Boes M, Cerny J, Massol R, Op dB, Kirchhausen T, Chen J, et al. T-cell engagement of dendritic cells rapidly rearranges MHC class II transport. *Nature.* 2002; 418:983–988. [PubMed: 12198548]
14. Mayordomo JI, Zorina T, Storkus WJ, Zitvogel L, Celluzzi C, Falo LD, et al. Bone marrow-derived dendritic cells pulsed with synthetic tumour peptides elicit protective and therapeutic antitumour immunity. *Nat Med.* 1995; 1:1297–1302. [PubMed: 7489412]
15. Lim DS, Kim JH, Lee DS, Yoon CH, Bae YS. DC immunotherapy is highly effective for the inhibition of tumor metastasis or recurrence, although it is not efficient for the eradication of established solid tumors. *Cancer Immunol Immunother.* 2007; 56:1817–1829. [PubMed: 17443323]

16. Chen XY, Zhang W, Zhang W, Wu S, Bi F, Su YJ, et al. Vaccination with viable human umbilical vein endothelial cells prevents metastatic tumors by attack on tumor vasculature with both cellular and humoral immunity. *Clin Cancer Res.* 2006; 12:5834–5840. [PubMed: 17020991]
17. Chow A, Brown BD, Merad M. Studying the mononuclear phagocyte system in the molecular age. *Nat Rev Immunol.* 2011; 11:788–798. [PubMed: 22025056]
18. Pflücke H, Sixt M. Preformed portals facilitate dendritic cell entry into afferent lymphatic vessels. *J Exp Med.* 2009; 206:2925–2935. [PubMed: 19995949]
19. Ohl L, Mohaupt M, Czeloth N, Hintzen G, Kiafard Z, Zwirner J, et al. CCR7 governs skin dendritic cell migration under inflammatory and steady-state conditions. *Immunity.* 2004; 21:279–288. [PubMed: 15308107]
20. Sato N, Ahuja SK, Quinones M, KostECKI V, Reddick RL, Melby PC, et al. CC chemokine receptor (CCR)2 is required for langerhans cell migration and localization of T helper cell type 1 (Th1)-inducing dendritic cells. Absence of CCR2 shifts the *Leishmania* major-resistant phenotype to a susceptible state dominated by Th2 cytokines, b cell outgrowth, and sustained neutrophilic inflammation. *J Exp Med.* 2000; 192:205–218. [PubMed: 10899907]
21. Stosel H, Koch F, Romani N. Maturation and migration of murine dendritic cells in situ. Observations in a skin organ culture model. *Adv Exp Med Biol.* 1997; 417:311–315. [PubMed: 9286379]
22. Lukas M, Stosel H, Hefel L, Imamura S, Fritsch P, Sepp NT, et al. Human cutaneous dendritic cells migrate through dermal lymphatic vessels in a skin organ culture model. *J Invest Dermatol.* 1996; 106:1293–1299. [PubMed: 8752673]
23. Tripp CH, Ebner S, Ratzinger G, Romani N, Stoitzner P. Conditioning of the injection site with CpG enhances the migration of adoptively transferred dendritic cells and endogenous CD8+ T-cell responses. *J Immunother.* 2010; 33:115–125. [PubMed: 20145551]
24. MartIn-Fontecha A, Sebastiani S, Hopken UE, Uguccioni M, Lipp M, Lanzavecchia A, et al. Regulation of dendritic cell migration to the draining lymph node: impact on T lymphocyte traffic and priming. *J Exp Med.* 2003; 198:615–621. [PubMed: 12925677]
25. Lesterhuis WJ, de Vries IJ, Adema GJ, Punt CJ. Dendritic cell-based vaccines in cancer immunotherapy: an update on clinical and immunological results. *Ann Oncol.* 2004; 15(Suppl 4):iv145–iv151. [PubMed: 15477299]
26. Prins RM, Craft N, Bruhn KW, Khan-Farooqi H, Koya RC, Stripecke R, et al. The TLR-7 agonist, imiquimod, enhances dendritic cell survival and promotes tumor antigen-specific T cell priming: relation to central nervous system antitumor immunity. *J Immunol.* 2006; 176:157–164. [PubMed: 16365406]
27. Ng CP, Hinz B, Swartz MA. Interstitial fluid flow induces myofibroblast differentiation and collagen alignment in vitro. *J Cell Sci.* 2005; 118:4731–4739. [PubMed: 16188933]
28. Chary SR, Jain RK. Direct measurement of interstitial convection and diffusion of albumin in normal and neoplastic tissues by fluorescence photobleaching. *Proc Natl Acad Sci U S A.* 1989; 86:5385–5389. [PubMed: 2748592]
29. Menon GK, Kollias N, Doukas AG. Ultrastructural evidence of stratum corneum permeabilization induced by photomechanical waves. *J Invest Dermatol.* 2003; 121:104–109. [PubMed: 12839570]
30. Jahnisch H, Fussel S, Kiessling A, Wehner R, Zastrow S, Bachmann M, et al. Dendritic cell-based immunotherapy for prostate cancer. *Clin Dev Immunol.* 2010; 2010:517493. [PubMed: 21076523]
31. Couzin-Frankel J. Immune therapy steps up the attack. *Science.* 2010; 330:440–443. [PubMed: 20966228]
32. Fong L, Brockstedt D, Benike C, Wu L, Engleman EG. Dendritic cells injected via different routes induce immunity in cancer patients. *J Immunol.* 2001; 166:4254–4259. [PubMed: 11238679]
33. O'Neill DW, Adams S, Bhardwaj N. Manipulating dendritic cell biology for the active immunotherapy of cancer. *Blood.* 2004; 104:2235–2246. [PubMed: 15231572]
34. Mosca PJ, Lysterly HK, Clay TM, Morse MA, Lysterly HK. Dendritic cell vaccines. *Front Biosci.* 2007; 12:4050–4060. [PubMed: 17485358]
35. Mullins DW, Sheasley SL, Ream RM, Bullock TN, Fu YX, Engelhard VH. Route of immunization with peptide-pulsed dendritic cells controls the distribution of memory and effector T cells in

lymphoid tissues and determines the pattern of regional tumor control. *J Exp Med.* 2003; 198:1023–1034. [PubMed: 14530375]

Translational relevance

Antigen-pulsed ex vivo matured dendritic cells (DCs) have been broadly evaluated for anti-tumor immunotherapy in the past two decades. Yet, efficacy of this DC-based immunotherapy is limited in part due to insufficient migration of injected DCs from the skin to draining lymph nodes following intradermal or subcutaneous injection. We show here that brief illumination of the inoculation site prior to intradermal inoculation of DCs with a safe, non-invasive laser greatly enhanced migration of the inoculated DCs from the skin to the draining lymph nodes. This translated into more vigorous expansion of antigen-specific cytotoxic T lymphocytes, complete suppression of early tumor growth, and prolonged survival of tumor-resected mice when compared to conventional DC-mediated immunotherapy. This simple, convenient laser-based approach merits further investigation for its use in improving DC-based immunotherapy in clinical settings.

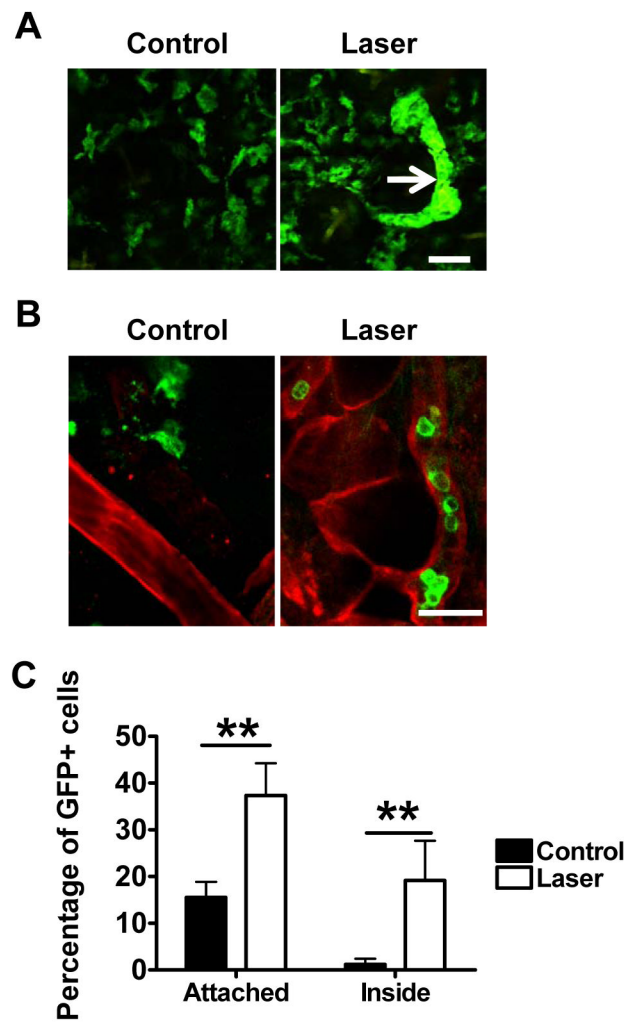


Figure 1. Laser facilitates lymphatic entry of dermal APCs

A. Formation of dermal cords after cutaneous laser illumination of MHC II-EGFP transgenic mice. Dermal GFP+ cells in the control (left) and laser-illuminated ear (right) are shown one hr after laser illumination. Arrow: dermal cords. Scale bar: 50 μ m. Experiments were repeated in three mice with similar findings. **B.** Representative images showing GFP+ cells inside LVs in laser-illuminated ear but not in control ear. Mouse ears were illuminated as in **A**, separated into two sheets 30 min later, and subjected to whole-mount collagen IV staining followed by the confocal microscopy imaging. Red, collagen IV; green, MHC II+ cells and scale bar, 25 μ m. Experiments were repeated in three mice with similar results. **C.** Percentages of GFP+ cells in association with LVs in the control (black) and laser-illuminated ear (white). Total ~250 GFP+ cells were counted in 15 randomly selected fields from three stained tissues in each group. **, $p < 0.01$.

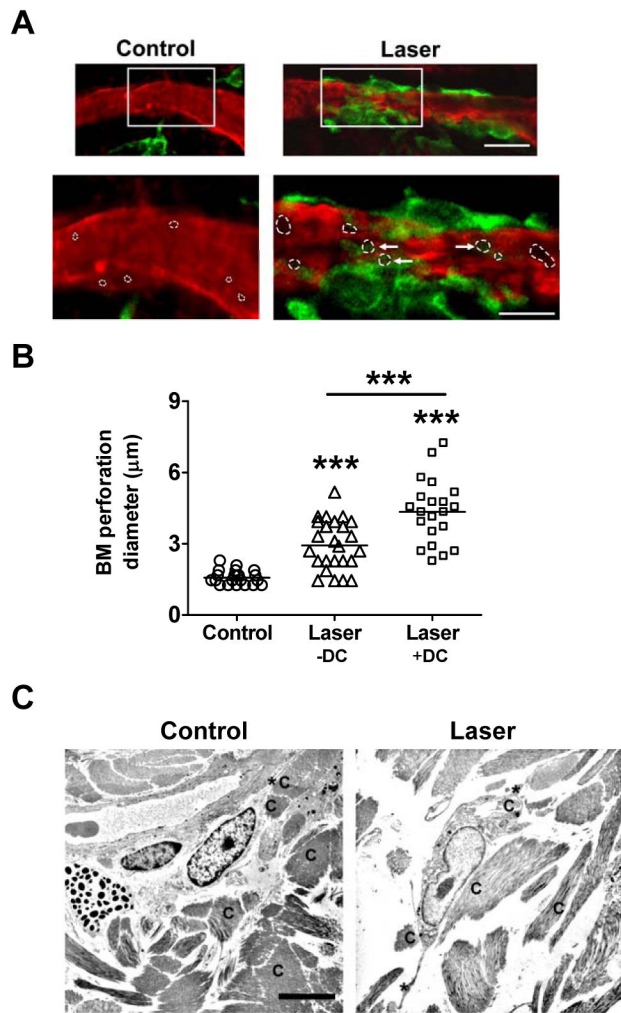


Figure 2. Laser enlarges perforations in the basement membrane of LVs

A. Laser induces adherence of APCs to LVs. Upper panel: Representative images showing distribution of GFP+ cells around LVs in collagen IV-stained whole-mount ear. Scale bar: 20 μm . Lower panel: Enlarged images of an indicated area (rectangle) in the upper panel. Perforations in the basement membrane were characterized as an unstained dark area and outlined by dotted white circles. Arrows point to perforations with cell occupancy. Scale bar: 10 μm . Experiments were repeated in at least three mice with similar findings. **B.** Laser enlarges basement membrane perforation. Six LVs were randomly selected from three stained ears for measurement of perforation diameters with or without cell occupancy. The data are presented by combined results from two investigators with one blinded to the sample identities. $n=21-26$ and ***, $p<0.001$. **C.** Laser modulates dermal scaffold. The low dorsal skin of BALB/c mice was exposed to laser illumination at 0.3W for 2 min, excised 30 min later, and subjected to transmission electron microscopy analysis. Non-treated control skin from the same mice was used as a control. Scale bar, 6 μm ; C, collagen fibers and *, cell dendrites. Similar findings were confirmed in at least three mice.

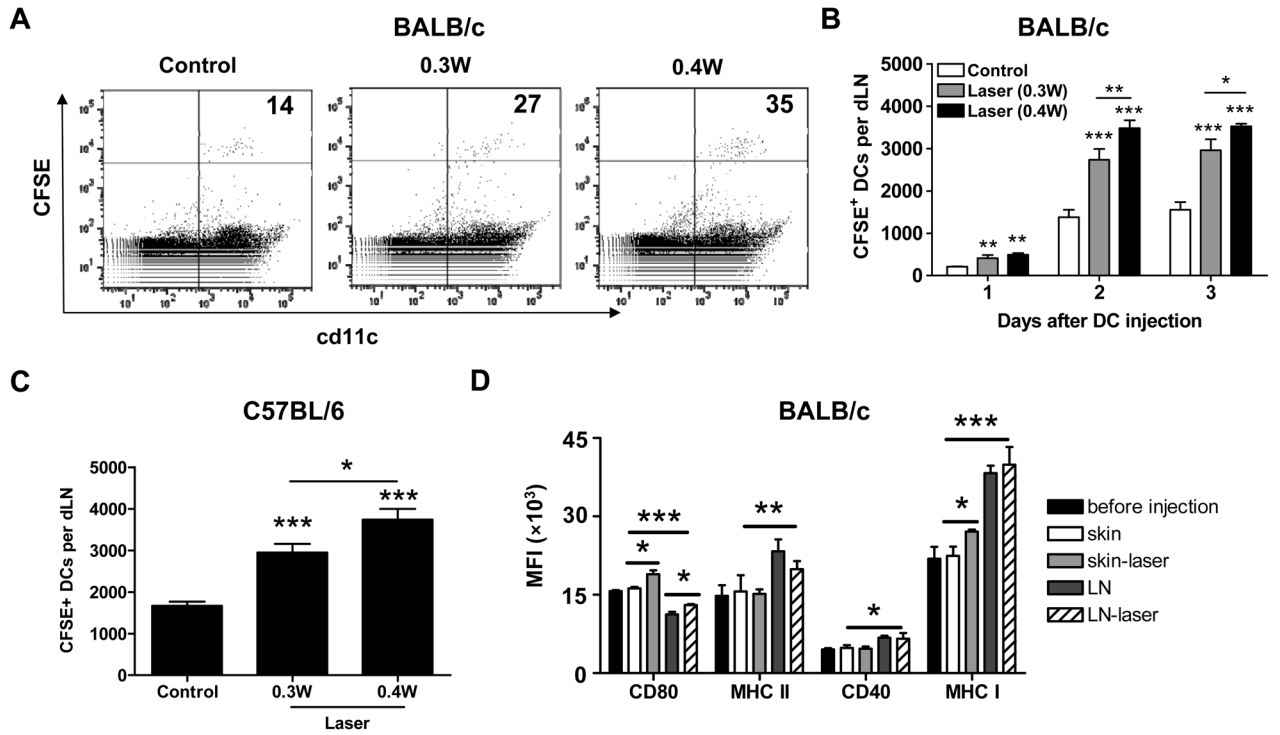


Figure 3. Laser enhances migration and maturation of *i.d.* injected mDCs

A–B. Laser enhanced DC migration in BALB/c mice. CFSE-labeled mDCs were *i.d.* injected to syngeneic BALB/c mice after laser or sham illumination at 0.3W for 2 min or at 0.4W for 1.5 min. Two days later, CFSE+cd11c+ DCs in the dLNs were quantified by flow cytometry and indicated in the upper right corner of the profile ($\times 100$) in **A** or averaged in **B**. Laser-enhanced earlier (day 1) and later (day 3) DC migration was also similarly quantified as shown in **B**. **C.** CFSE-labeled mDCs from B6.SJL mice were *i.d.* injected to congenic C57BL/6 (B6) mice and CFSE+cd11c+ cells in the dLNs were calculated on day 2 after DC injection. **D.** In a second experiment, single cells of the skin and dLNs were immunostained and subjected to flow cytometry analysis of expression of costimulatory molecules (CD80, MHC II, CD40 and MHC I) two days after mDC injection to BALB/c mice. Mean fluorescence intensity (MFI) of these markers was shown. $n=6$; *, **, ***, $P<0.05$, 0.01, 0.001, respectively. Experiments were repeated twice with similar results.

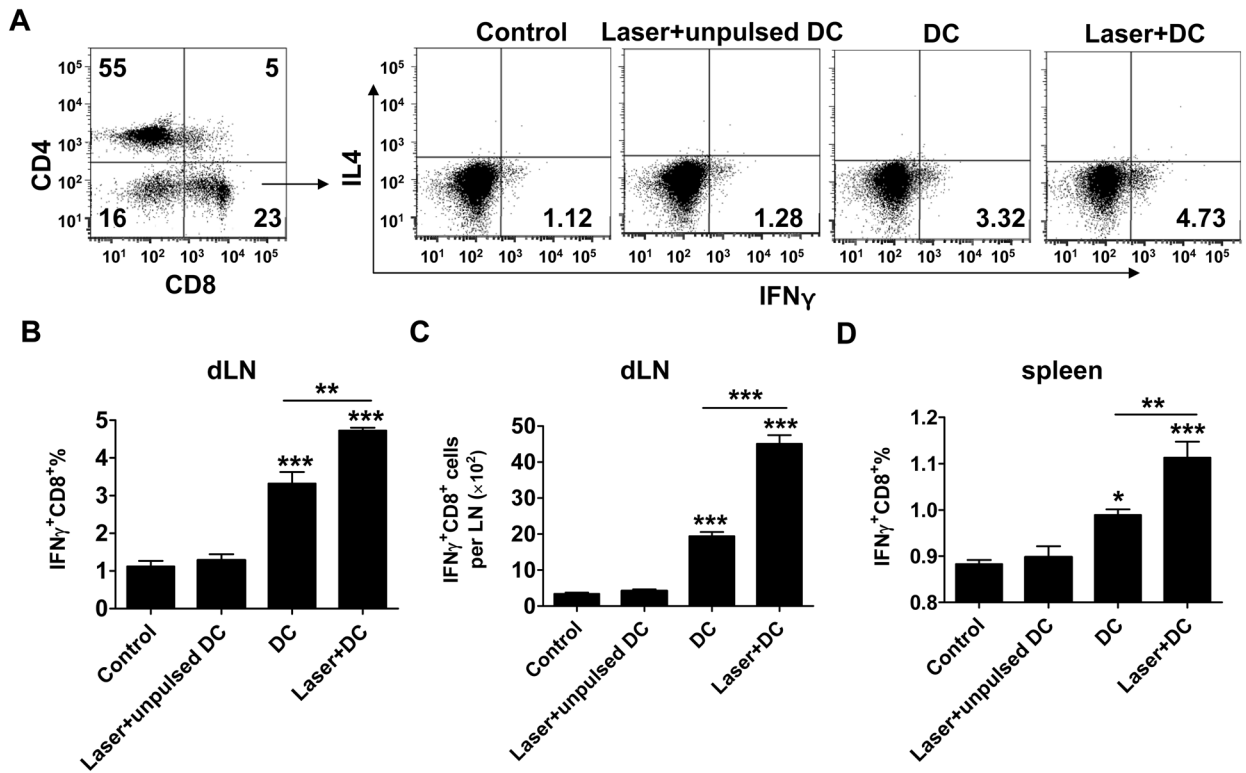


Figure 4(A-D)

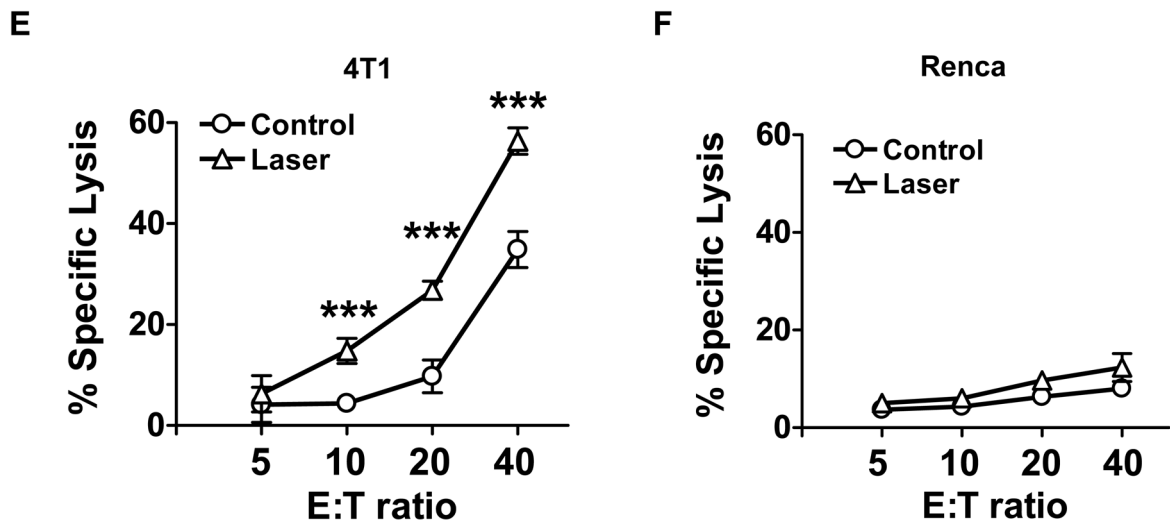


Figure 4(E-F)

Figure 4. Laser expands tumor specific CD8⁺ cells

One week after three immunizations of 4T1 tumor lysate-pulsed mDCs in BALB/c mice with or without laser, cells in the dLNs were isolated and analyzed for IFN γ -secreting CD8⁺ T cells. Representative flow cytometry profiles show the percentages of IFN γ -secreting CD8⁺ T cells in the dLNs (**A**). Percentages of IFN γ -secreting CD8⁺ T cells in the dLNs and the spleen are summarized in (**B**) and (**D**), respectively, and the number of IFN γ -secreting CD8⁺ T cells per dLN is given in **C**. **E–F**. T lymphocytes isolated from similarly immunized mice as above were stimulated with mitomycin C-treated 4T1 tumor cells, and incubated with 4T1 tumor cells (**E**) or irrelevant Renca cells (**F**) in triplicate at different E:T ratios. Lactate dehydrogenase released was quantified by non-radioactive assays and percentages of specific killing were shown. n=6; *, **, ***, P<0.05, 0.01, 0.001, respectively. Experiments were representative of three experiments.

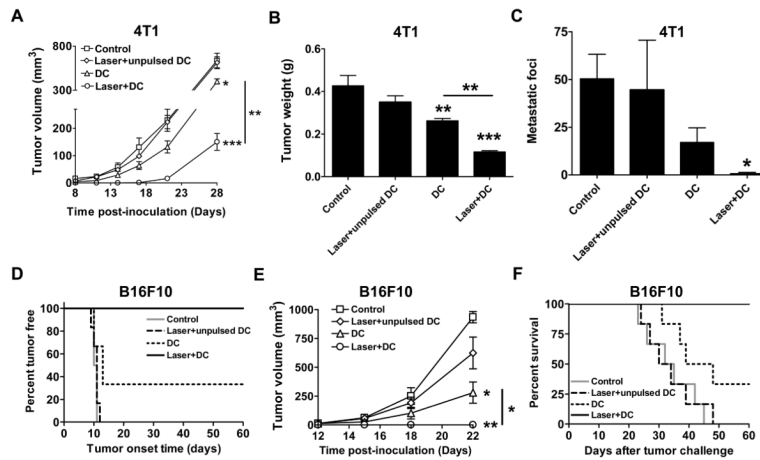


Figure 5. Laser suppresses tumor growth

A–C. Suppression of 4T1 tumor growth in BALB/c mice. 4T1 tumor volume (**A**), weight (**B**), and metastatic foci (**C**) were compared among the groups. Lung metastatic foci were counted under a dissection microscope. **D–F.** Suppression of B16F10 melanoma growth in C57BL/6 mice. Tumor outgrowth (**D**) and survival of tumor-bearing mice (**F**) were monitored for 60 days and tumor growth (**E**) was monitored for ~3 weeks. $n=6$; *, **, ***, $p<0.05$, 0.01, 0.001, respectively. Experiments were repeated twice with similar results.

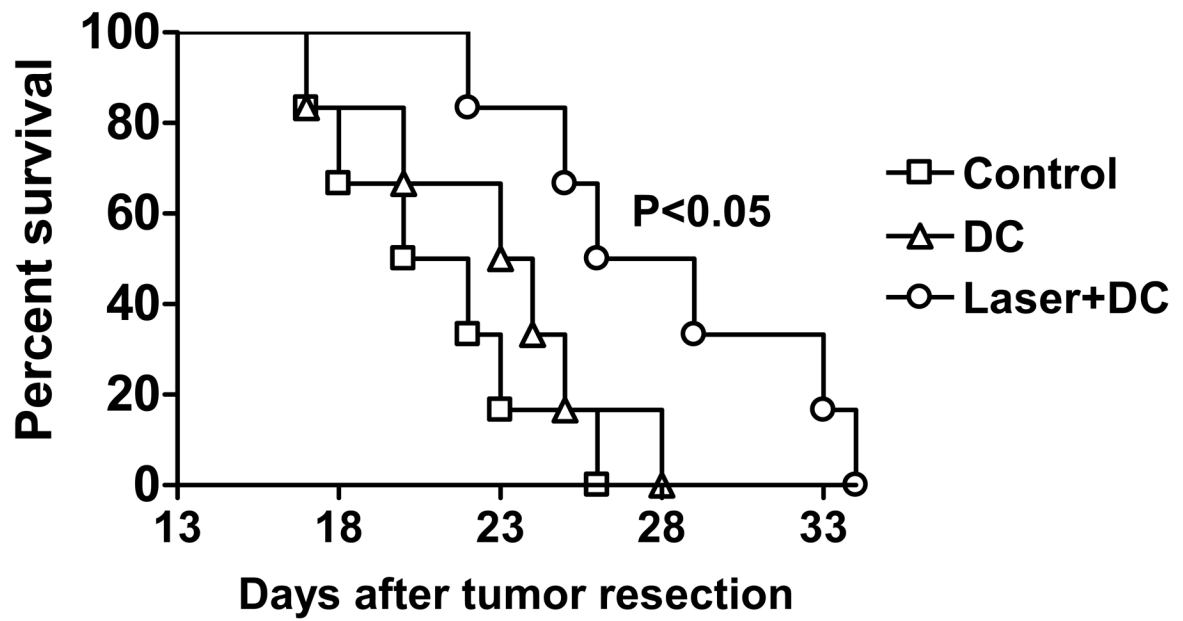


Figure 6. Laser extends the survival of tumor-resected mice

Kaplan-Meier curve shows the survival of tumor-resected mice. Tumor-resected BALB/c mice were *i.d.* immunized with PBS (control), 4T1 tumor lysate-pulsed mDCs without laser (DC) or with laser (laser+DC) once a week for three weeks. Survival of tumor-resected mice was monitored. $n=6$. Experiments were repeated twice with similar results.